Biomechanical Impact Response of the Human Chin and Manubrium

Jason A. Stammen,[1] John H. Bolte IV,[2] and Joshua Shaw[3]

[1]National Highway Traffic Safety Administration, East Liberty, OH, USA; [2]The Ohio State University, Columbus, OH, USA; and [3]Transportation Research Center, East Liberty, OH, USA

Associate Editor Stefan M. Duma oversaw the review of this article.

Abstract—Chin-to-chest impact commonly occurs in frontal crash simulations with restrained anthropomorphic test devices (ATDs) in non-airbag situations. This study investigated the biofidelity of this contact by evaluating the impact response of both the chin and manubrium of adult post-mortem human subjects (PMHSs). The adult PMHS data were scaled to a 10-year-old (YO) human size and then compared with the Hybrid III 10YO child (HIII-10C) ATD response with the same test configurations. For both the chin and manubrium, the responses of the scaled PMHS had different characteristics than the HIII-10C ATD responses. Elevated energy impact tests to the PMHS mandible provided a mean injury tolerance value for chin impact force. Chin contact forces in the HIII-10C ATD were calculated in previously conducted HYGE sled crash simulation tests, and these contact forces were strongly correlated with the Head Injury Criterion ($HIC_{36\ ms}$). The mean injurious force from the PMHS tests corresponded to a $HIC_{36\ ms}$ value that would predict an elevated injury risk if it is assumed that fractures of the chin and skull are similarly correlated with $HIC_{36\ ms}$. Given the rarity of same occupant-induced chin injury in booster-seated occupants in real crash data and the disparity in chin and manubrium stiffnesses between scaled PMHS and HIII-10C ATD, the data from this study can be made use of to improve biofidelity of chin-to-manubrium contact in ATDs.

Keywords—Biomechanics, Chin, Manubrium, Biofidelity, Head injury.

INTRODUCTION

Chin-to-chest impact frequently occurs in frontal crash simulations with anthropomorphic test devices (ATDs). The lack of thoracic spine flexibility, limited neck elongation, and shoulder rigidity in some ATD designs can cause exaggerated neck flexion, with the head rotating such that the chin contacts the sternum area of the ATD. While interaction of either the chin or face with the chest has been shown to occur in both adolescent and adult human subject experimental crash simulation studies,[1,6,7,13] the existence of injuries due to this type of contact in real world crashes is rare. A search of 1999–2008 National Automotive Sampling System data was conducted for all AIS 2–6 head or face injuries sustained by occupants not seated in the front seat (no frontal airbag interaction) with a principal direction of force (PDOF) equal to 11, 12, or 1 o'clock (purely or near-purely frontal crash) where the most severe vehicle damage was not attributed to rollover.[11] This search revealed 812 AIS 2 + head and face injuries, but none was attributed to chin–chest contact.

While there is a lack of head/face injury due to chin–chest contact in accident data, this type of contact does occur in ATD testing, and it can result in high head accelerations in some test scenarios. This can lead to difficulty in assessing head injury risk, which is typically done by calculating the Head Injury Criteria ($HIC_{36\ ms}$).[10] One test scenario illustrating this difficulty is FMVSS No. 213-type belt-positioning booster seat testing with the Hybrid III 10-year-old (YO) child (HIII-10C) ATD.[11,16] This testing showed that posture and booster design can alter the severity of chin-to-chest contact.

The objective of this study was to evaluate dummy design factors for their effect on head accelerations from chin contact in booster seat testing conducted by the National Highway Traffic Safety Administration (NHTSA) Vehicle Research & Test Center (VRTC). The first part of this study compared scaled adult post-mortem human subject (PMHS) and HIII-10C ATD chin responses at sled test-level chin impact energies. The second part of this study investigated the upper chest (manubrium) of adult PMHS and the HIII-10C ATD. Finally, adult PMHS chins (mandibles) were impacted at elevated energies to determine the force

Address correspondence to Jason A. Stammen, National Highway Traffic Safety Administration, East Liberty, OH, USA. Electronic mail: jason.stammen@dot.gov

level at which injury is caused in adults, and these data were then analytically related to the chin-contact forces observed in HIII-10C booster seat tests.

MATERIALS AND METHODS

Experimental impact tests were conducted on the chin and manubrium of adult PMHS and the HIII-10C ATD. The experimental impact energy was derived by applying conservation of impulse-momentum to HYGE sled crash simulation test data.

Chin Impact Response

The chin contact forces observed in FMVSS No. 213 booster seat sled tests with the HIII-10C dummy (Table 1) were resolved using force–time histories that included X and Z components.

The Y components were ignored because the motion due to chin contact is almost purely in the X–Z plane (Fig. 1). Using a combination of chalk transfer location and pressure tape markings on the lower neck/spine box in HYGE sled tests, along with high-speed video from modified neck pendulum tests with the chest jacket removed (Fig. 2), the location of the chin force application was determined. Because the chin surface area is so small, the impact probe diameter of $2''$ (surface area $= 2027$ mm^2) was used to fully encompass the chin area typically in contact with the chest in HYGE sled testing.

Rigid body motion was assumed for this analysis. The force equations (assuming all motion is in the X–Z plane) were therefore

$$m_{\text{head}} * a_{\text{head}(x)}(t) = F_{\text{chin}(x)}(t) + F_{\text{neck}(x)}(t)$$

$$m_{\text{head}} * a_{\text{head}(z)}(t) = F_{\text{chin}(z)}(t) + F_{\text{neck}(z)}(t)$$

TABLE 1. FMVSS No. 213 booster seat tests (from Stammen and Sullivan[16]).

Test number	Belt positioning booster	HIC$_{36\text{ ms}}$	Posture/torso angle (°)	Peak chin XZ contact force (N)	Chin contact velocity (m/s)	*Change in momentum/impulse (N s)
314-2	Evenflo Generations	1216	19.4	5895	3.96	16.2
314-2	Evenflo Generations	622	15.0	2581	3.81	22.4
315-2	Compass 500	1524	20.2	6964	6.47	36.8
315-2	Compass 500	792	15.0	3203	5.04	61.0
315-3	Graco Cherished Cargo	1126	19.4	5944	4.66	24.4
315-3	Graco Cherished Cargo	773	19.8	3936	4.47	35.2
327-2	Combi Kobuk	989	13.7	2611	3.94	20.6
327-1	Combi Kobuk Sport	808	15.4	4467	3.93	32.3
327-1	Recaro Young Sport	931	17.1	4416	4.84	44.3
323-1	Evenflo Chase Premiere	839	15.6	4797	3.45	12.5
324-1	Safety 1st Vantage Point	911	17.1	4563	4.08	25.3

*Using physical head mass and chin contact velocity.
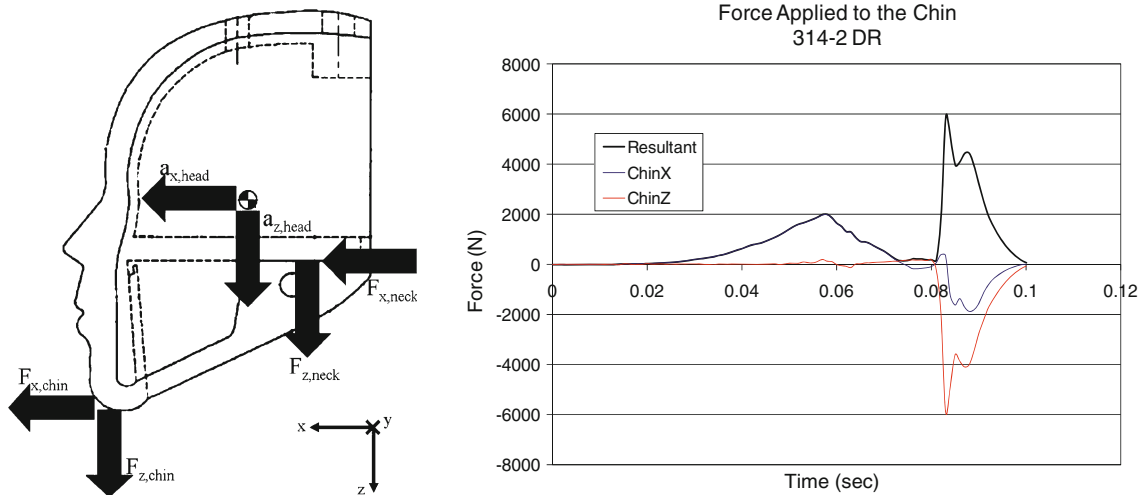
FIGURE 1. Free body diagram of chin contact and chin force–time history example.
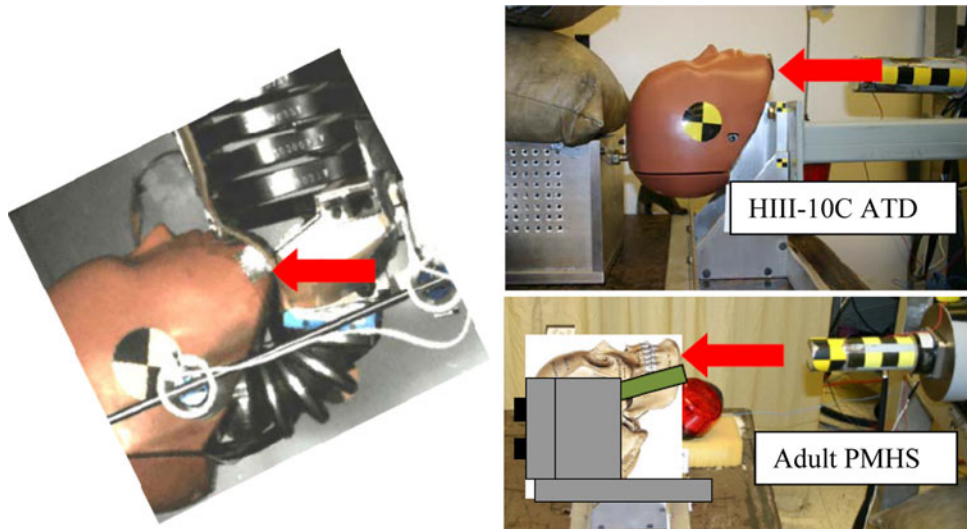
FIGURE 2. (Left) Modified pendulum test showing HIII-10C ATD chin relative to chest at the time of contact as would be observed in a sled test (picture shown upside down to relate to experimental setup); (right) experimental test setup for chin impact tests.

Solving these equations for the x and z components of F_{chin} gave

$$F_{chin(x)}(t) = m_{head} * a_{head(x)}(t) - F_{neck(x)}(t)$$

$$F_{chin(z)}(t) = m_{head} * a_{head(z)}(t) - F_{neck(z)}(t)$$

The time history of the resultant chin force was then calculated to be

$$F_{chin(xz\ resultant)}(t) = \sqrt{F_{chin(x)}(t)^2 + F_{chin(z)}(t)^2}$$

where each exponent is applied to each element in the time series. To compare the ATD and PMHS responses, a linear impact was to be applied to the z axis of a fixed head with a 24-kg probe. The z-axis loading direction was chosen because it was observed in the chin force–time histories (Fig. 1) that the z force component dominates the chin response and is very close to the resultant XZ force during the impact phase (80–90 ms). In addition, artificial rotational effects were minimized because the bottom of the chin is more flat on the inferior surface. The velocity required to replicate the impulse sustained by the HIII-10C's chin in a sled test having a severe chin-to-chest contact (test 315-2 with $HIC_{36\ ms} = 1524$ in Table 1) was calculated using the conservation of impulse-momentum:

$$\int_{t(V_{initial})}^{t(V=0)} F_{chin(xz\ resultant)}(t)dt$$

$$= m_{probe} * \Delta V_{probe(xz\ resultant)}$$

$$= m_{probe} * \left(0 - V_{probe(xz\ resultant)}\ \text{at contact}\right)$$

where $t(V_{initial})$ is the time at initial chin–chest contact, and $t(V = 0)$ is the time where the chin skin is fully compressed and the chin is changing direction to rebound.

$$V_{probe(xz\ resultant)} = \int_{t(V_{initial})}^{t(V=0)} F_{chin(xz\ resultant)}(t)dt/m_{probe}$$

$$= 36.8\,\text{N s}/24\,\text{kg} = 1.54\,\text{m/s}$$

Noting that the chin-contact velocities in the sled tests were much higher than this speed, the calculated impact velocity was rounded to a nominal speed of 1.6 m/s, and the kinetic input energy was calculated using the probe mass and the calculated impact velocity:

$$E = 1/2\,m_{probe} * V^2_{probe(xz\ resultant)}$$

$$= 1/2(24\,\text{kg}) * (1.6\,\text{m/s})^2 = 30.7\,\text{J}$$

Therefore, using neck force and head acceleration data from a sled test having typical chin-to-manubrium contact, the kinetic input energy was found to be 30.7 J, which equates to an impact velocity of 1.6 m/s for a 24 kg probe mass. Fixtures to hold both HIII-10C heads and adult PMHS[1] heads for chin impact tests were designed and fabricated. The HIII-10C fixture included a rigid attachment at the occipital condyle with a physical stop to prevent rotation and a

---

[1]The PMHS were available through the body donor program at The Ohio State University's Injury Biomechanics Research Laboratory, and applicable NHTSA guidelines as well as IRB protocol were followed.

TABLE 2. Subject characteristics for chin testing.

Subject	Age	Gender	Head width (mm)	Head circumference (mm)	Head height (mm)	Head length (mm)
CHN2	91	F	142	552	212	189
CHN3	78	M	153	600	250	201
CHN4	46	M	160	600	236	204
CHN5	66	M	161	588	226	177
CHN7	50	M	139	554	227	188
CHN8	47	M	155	620	182	210
CHN9	80	M	161	585	222	185
Avg.	65.4		153	586	222	193
Std. Dev.	18.2		9.1	24.9	21.3	11.8
H3-10C[a]			168		183[b]	208

[a]From dimensions listed in head assembly drawings.
[b]From forehead to rearmost portion of headform.

tension member to prevent translation and bending of the fixture, while the adult PMHS fixture had reaction surfaces for the sides and top of the head. The anatomical z-axis of the head was aligned with the direction of impact. Care was taken to orient the HIII-10C and adult PMHS relative to the ram (Fig. 2) such that all the impact energy generated by the ram was applied through the anatomical z-axis to the chin. This configuration simulates the relative orientation of the chin and upper chest structure of the HIII-10C in a typical chin–chest contact. The anthropometry of each adult PMHS was measured (Table 2), and major landmarks on the mandible, skull, and fixture were marked with targets for high-speed video analysis. The adult PMHS head was then fixed in place using multiple screws through the skull on the top and side reaction surfaces. All fixture connections were superior to the temporomandibular joint (TMJ) so that the joint was allowed to compress during the impact. The jaw was closed using a chin strap that ran across the bottom of the mandible spanning the side reaction plates to ensure that all displacement was through tissue compression in the mandible, facial bones, upper/lower dentition, and TMJ. All subjects had intact dentition and were screened for osteoporosis and jaw disorders.

Tests were conducted at a nominal speed of 1.6 m/s on two HIII-10C ATD headforms, one each manufactured by FTSS (First Technology Safety Systems) and Denton ATD. Two repeat tests were conducted on each headform with more than 30 min between the repeats. Before testing, the chin skin of each headform was measured for thickness and durometer. During the test, ram acceleration, force, and displacement were measured so that stiffness could be calculated. Tests were then done on seven adult PMHS, with the same channels being measured as in the HIII-10C tests. Three tests were conducted on each adult PMHS. The first test was done at approximately 25% of the input energy (0.8 m/s) to exercise the mandible and provide a

baseline response for injury identification. The second test was done at full energy (1.6 m/s). A third and final test was then done at 25% energy to compare to the first test. If the first and third test responses were consistent, no injury was anticipated but the final assessment was not made until post-test CT and autopsy.

Affixed to the probe were a linear variable differential transformer (LVDT) to measure displacement, a uniaxial accelerometer to measure acceleration, and a six-axis load cell to measure forces and moments. The displacement, acceleration, and force channels were acquired at 20 kHz and filtered per SAE J211 procedure. The data channel bias was removed at time zero (determined by initial contact with the chin) and shifted in time to the point of initial rise (using a 25-N threshold for HIII-10C and high-energy PMHS impacts, and 0.5-g threshold for low-energy PMHS impacts) to account for residual differences in the degree of jaw closure after strapping the jaw shut. The force channel was inertially compensated for the additional mass of the impact face in front of the load cell attached to the probe. A force–displacement corridor was generated from the PMHS data using the two-dimensional ellipse method introduced by Shaw *et al.*[14] Stiffness was calculated in two ways because of the nonlinear behavior. The first approach used the force (F) and displacement (x) data up to the maximum displacement ($x_{(max)}$) and solved the potential energy equation for K:

$$K = \frac{2 \int_0^{x_{(max)}} F(x)dx}{x_{(max)}^2}$$

The maximum displacement was used instead of the maximum force because only the loading portion of the curve would contribute to the stiffness calculation. In this way, no portion of the rebound phase would contribute to the stiffness. The second stiffness

calculation method used a straight-line calculation between 10 and 90% of the peak force with the associated displacement values at those force locations:

$$K = \frac{(F_{90\%} - F_{10\%})}{(X_{F90\%} - X_{F10\%})}$$

This method accounted for any toe-in region caused by interfacial effects during the initial contact phase between the impactor and chin.

Chin Fracture Tolerance

The chin injury portion of this study was completed on four of the seven PMHS (the initial series of three PMHS were evaluated for response only) using the same setup and methodology as the aforementioned adult PMHS dynamic chin testing. However, the input energy was increased at set intervals by increasing the impact velocity (equivalent to nominally 150% of the previous test energy) up to a point where injury was believed to have occurred. Injury was verified by repeating a baseline energy test at 0.8 m/s after each elevated energy impact. If the repeat baseline test response after an elevated energy test showed a significant change in shape, amplitude, or phase, then the testing was stopped as injury was assumed. While it was assumed that the baseline energy impact conducted after the fracture-inducing impact did not appreciably change the fracture patterns, injury severity and pattern were not the focus of this study but rather whether or not AIS 2+ injury occurred. Moreover, the response curve for each elevated energy test was examined after the impact was administered, and often this curve showed indications of injury. The specimen was examined post-test for injuries.

Manubrium Impact Response

The other half of the chin-to-chest contact is the impact response of the upper sternum/manubrium (of adult PMHS) or the upper chest/lower neck area (of the HIII-10C dummy). Therefore, it was desirable to determine the response characteristics of this area as a result of impact by the chin. To eliminate the variability encountered in PMHS chins, a rigid probe having the mass of a HIII-10C head (3.73 kg) and impact face diameter replicating the cross-sectional area of the chin (2027 mm^2) was fabricated. This probe was then dropped onto the upper chest of the HIII-10C and upper sternum (manubrium) of six PMHS. To represent the same 30.7 J input energy as the chin impacts, the probe was suspended at 839 mm above the impact site and then released by cutting the string holding it for a nominal impact velocity of 4.0 m/s.

The impacted object, HIII-10C or PMHS, was positioned such that the point of impact was level with the ground using an adjustable incline and perpendicular to the path of the falling probe. Both the incline and PMHS/ATD were secured to the test table to prevent sliding of the PMHS/ATD down the incline during the test. High-speed video as well as linear acceleration of the probe and triaxial acceleration of the manubrium were recorded. Figure 3 shows an overview of the testing setup. The linear acceleration of the probe was multiplied by its mass to get force and double-integrated to get displacement. Table 3 summarizes the subject characteristics.
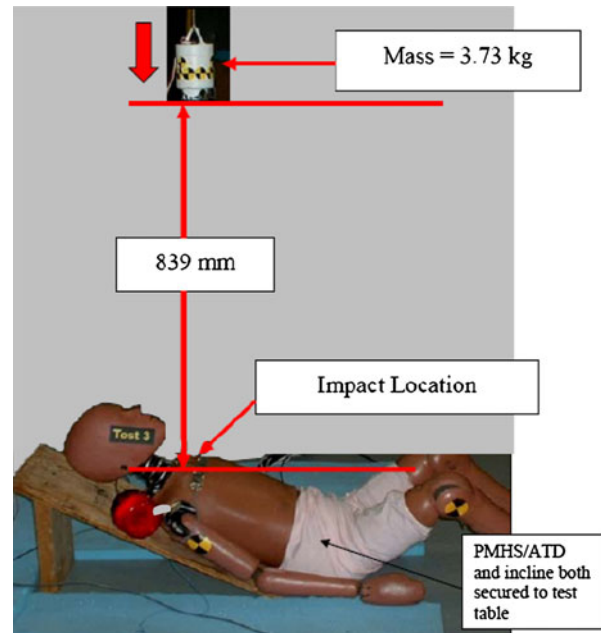

FIGURE 3. Dynamic upper sternum test setup for HIII-10C and adult PMHS.

TABLE 3. Subject characteristics for upper chest testing.

Subject	Age	Gender	Shoulder breadth (mm)	Chest breadth (mm)	Chest circumference (mm)	Chest depth (mm)
STM1	65	M	356	298	965	217
STM2	72	M	352	360	1175	247
STM3	63	M	355	299	978	194
STM4	50	M	320	298	1030	141
STM5	47	M	384	279	965	213
STM6	80	M	348	270	980	185
Avg.	63		353	301	1016	200
Std. Dev.	12.6		20.4	31.5	81.8	35.8
HIII-10C[a]			315	213	704	191

[a]From dimensions listed in external dimension drawing (420-0000, NHTSA-2005-21247)[4].

Scaling

The force and deflection data from adult PMHS chin and upper chest data were scaled to represent a 10YO-sized human using methods described in Mertz et al.[9] The equations for scaling force and deflection based on stiffness and mass ratios are

$$R_F = \lambda_V \sqrt{\lambda_{me} \lambda_k}$$

$$R_D = \lambda_V \sqrt{\lambda_{me} / \lambda_k}$$

where λ_V is the impact velocity scale factor, λ_{me} is the equivalent mass scale factor (for drop tests this is the ratio of relevant masses; i.e., the pendulum mass), and λ_k is the stiffness scale factor.

For the present study, the impact velocity scale factor, λ_V, is equivalent to unity since all impacts, either sternum (4.0 m/s) or chin (1.6 m/s), were conducted at within 0.1 m/s of the nominal velocity for both ATD and PMHS. Also, the equivalent mass scale factor, λ_{me}, is set to unity since all impacts, either sternum (3.73 kg) or chin (24 kg), were conducted with the same mass across all ATD and PMHS. The stiffness scale factor is

$$\lambda_k = \lambda_E \lambda_L$$

where λ_L is the characteristic length scale factor, and λ_E is the bone modulus scale factor (equivalent to 0.854 between adult and 10YO, see Mertz et al.[8]).

These equations apply for all body regions; however, the characteristic length scale factor should be chosen using engineering judgment. For example, the sternum impact data should be scaled by an appropriate dimension along the line of action such as chest depth. Likewise, the chin data should be scaled by head length (chin to top of head). Therefore, the characteristic length scale factors for these two tests are

$$\lambda_L = \lambda_X = \frac{\text{ChestDepth}_{10YO}}{\text{ChestDepth}_{\text{Subject}}} \text{ for the sternum tests, and}$$

$$\lambda_L = \lambda_Z = \frac{\text{HeadLength}_{10YO}}{\text{HeadLength}_{\text{Subject}}} \text{ for the chin tests.}$$

RESULTS

Figure 4 shows the processed force–deflection responses for the two HIII-10C headskins. There is a force required to move the chin skin (remove the clearance between the inside surface of the chin skin and the outside surface of the skull casting) before compression of the chin skin. Since the headskin is a one-piece component that is in some level of membrane
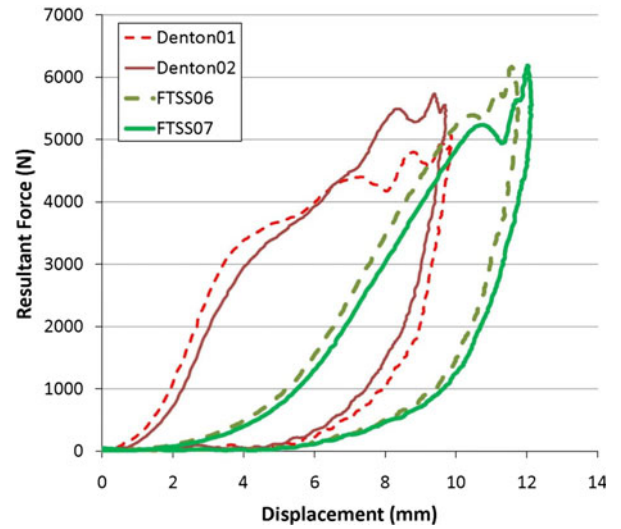

FIGURE 4. HIII-10C dummy force–deflection responses in chin impacts.

tension from covering the entire skull casting, there is some initial resistance to translation.

Figure 5 shows the un-scaled and scaled responses for the seven adult PMHS heads tested. In this case, the initial peak in force is less pronounced than in the HIII-10C. The initial peak is due to inertial resistance of the mandible mass before compression of soft tissue and skeletal structures. Fixture displacement due to impact was typically less than 2.5 mm for PMHS tests and less than 1 mm for ATD tests. A summary of the results is found in Table 4.

None of the subjects shown in Fig. 5 experienced injury at the 30.7 J input energy. Subjects CHN5, CHN7, CHN8, and CHN9 were re-tested at higher energies and did sustain injury. Figure 6 depicts the response curves of the four PMHS chins tested to failure which show a distinct change in response believed to be the point of failure. An average scaled-to-10YO size impact force of 4897 ± 1258 N was associated with fracture to the mandible or other facial bones (Table 5).

The injuries observed in these tests were AIS 1–2 in severity and included maxilla, mandible, and LeFort I and II fractures as well as a TMJ dislocation. Locations and descriptions of these injuries for each subject are shown in Fig. 7.

Figure 8 shows the manubrium force vs. deflection responses of the HIII-10C ATD and PMHS tested. No manubrium injuries were found in post-test examination.

The peak responses for the dynamic manubrium impact tests are shown in Table 6.

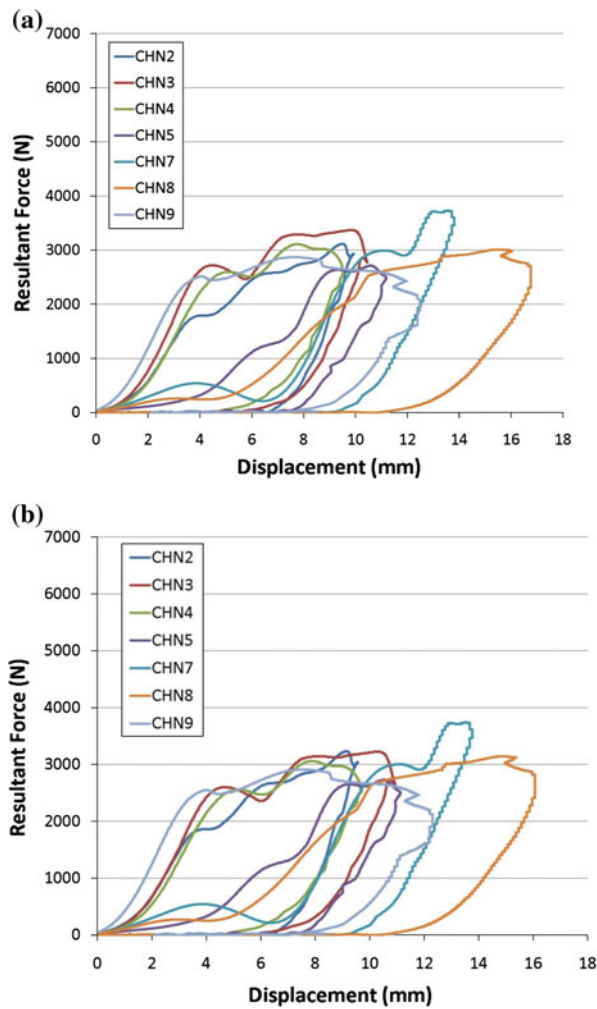Figures 9 and 10 show the PMHS corridors vs. ATD response for the chin and manubrium, respectively.

FIGURE 5. (a) Un-scaled PMHS responses in chin impacts. (b) Scaled PMHS responses in chin impacts.

DISCUSSION

To determine the degree of stiffness overlap between PMHS and HIII-10C, a response corridor was derived for the scaled PMHS and compared with the HIII-10C chin impact data (Fig. 9). The plot shows that the loading portions of the PMHS and ATD responses overlap some, but there is more area between the loading and unloading curves (hysteresis) in the PMHS than in the ATD. This can be illustrated by the rebound of the impact probe following the impact in video analysis. The probe "springs" back at a higher velocity in the HIII-10C test than it does in the PMHS test. This behavior indicates that a smaller percentage of the kinetic energy from the impact is lost in the HIII-10C than in the PMHS.

The difference in peak forces for ATD headskin (5.8 kN) and scaled PMHS chin (3.1 kN) is consistent with previous study by Craig et al.,[3] where they found similar differences in 25 J chin impacts to the Hybrid

III 50th chin compared to PMHS (peak forces averaged 5.5 vs. 3.7 kN). The FTSS headskin of the HIII-10C was closer to the scaled PMHS stiffness (potential energy-based) and peak displacement than the Denton headskin. Given the durometer (36.8) and thickness (10.7 mm) of the FTSS chin, it appears that these values could be used as a starting point for a chin thickness specification of the HIII-10C headskin. However, the peak forces in the Denton headskin were lower than the FTSS headskin. It appears that this peak force is sensitive to the very small differences in motion of the fixture and skull casting at the end of forward ram displacement, as the skin compression has reached its maximum limit before displacement ceases. Given the stiffer and thinner Denton headskin, more energy would remain to cause fixture/skull motion at the end of the event, which would limit the reaction force somewhat. It also can be observed in Fig. 9 that the FTSS headskin has a longer "toe-in" region than the Denton headskin. The fit of the headskins to their respective skull castings was not appreciably different, which indicates that the impact/shock resistance of the headskins, perhaps due to durometer, was the primary factor causing this "toe-in" difference. Regardless of these ATD headskin differences, a narrowed tolerance for these durometer/stiffness values would improve chin-to-chest impact response consistency for the HIII-10C assuming similar kinematics.

The manubrium force–displacement curves for the HIII-10C and PMHS were quite different in shape from one another (Fig. 10), and the second phase of the curve in the HIII-10C response had a much higher stiffness than the PMHS. It is this second slope that contributes to the head acceleration spike due to chin contact observed in HYGE sled testing. The HIII-10C dummy's manubrium was softer than the scaled PMHS manubrium up until around 40 mm of displacement, followed by an abrupt increase in force due to contact with the rigid ATD understructure. The HIII-10C peak force (3510 N) was over three times that of the PMHS average (1004 ± 155 N). In order to match the PMHS-derived manubrium force–displacement curve, the HIII-10C's upper chest would have to be made such that (a) the peak force is reduced significantly, and (b) the force should begin to rise at a lower deflection. It appears that there is not enough initial resistance in the chest structure to prevent the chin from penetrating into the deeper, more rigid structures in the ATD chest.

The scaling techniques employed to create the corridors for the 10YO ATD assume that the stiffness ratio of a 10YO to a 50th percentile adult is a constant value, when it is known that factors, such as age and osteoporosis, influence bone strength and stiffness. If those factors were taken into account for the PMHS

TABLE 4. Chin impact test summary (PMHS data scaled to 10YO size).

10YO ATD headskin ID or PMHS	Dimensional[a]		Fixed-head impact					
	Thickness (mm)	Durometer	Peak force (N)	Dx at peak force (mm)	Peak Dx (mm)	Force at peak Dx (N)	Potential energy stiffness (N/mm)	10–90% stiffness (N/mm)
CHN2			3114	9.44	9.92	2930	364	353
CHN3			3368	9.70	10.5	2770	427	511
CHN4			3110	7.69	9.54	2570	406	470
CHN5			2720	10.5	11.2	2490	202	445
CHN7			3730	13.5	13.8	3600	196	297
CHN8			3010	15.3	16.8	2700	181	332
CHN9			2870	7.42	12.5	2090	349	476
PMHS Avg.			3132	10.5	12.0	2736	304	412
PMHS Std. Dev.			334	2.9	2.6	464	107	83
Dentonchin01	7.1	57.1	5064	9.9	9.9	5042	618	576
Dentonchin02	7.1	57.1	5735	9.4	9.7	5464	626	758
FTSSchin06	10.7	36.8	6169	11.6	11.8	5251	375	748
FTSSchin07	10.7	36.8	6187	12.0	12.1	5556	369	714
ATD Avg.			5789	10.7	10.9	5328	497	699
ATD Std. Dev.			526	1.3	1.2	230	144	84

[a]The current durometer specification for the 10YO headskin is Shore A 35–45. There is no current specification for the thickness of the headskin chin area.
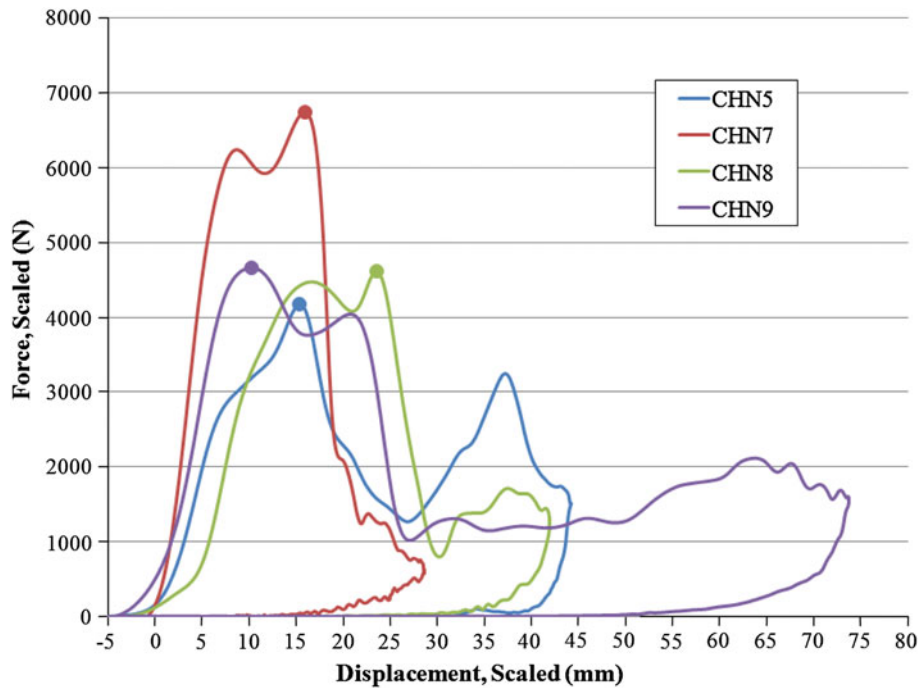
FIGURE 6. Chin impact force vs. displacement—PMHS elevated energy tests.

tested in this study, then the corridors would be expected to have larger standard deviation. In addition, chest depth and head length were assumed to be appropriate for the characteristic length scale factor. It is possible that different anthropometric parameters would be more appropriate for the loading configurations exhibited in this study.
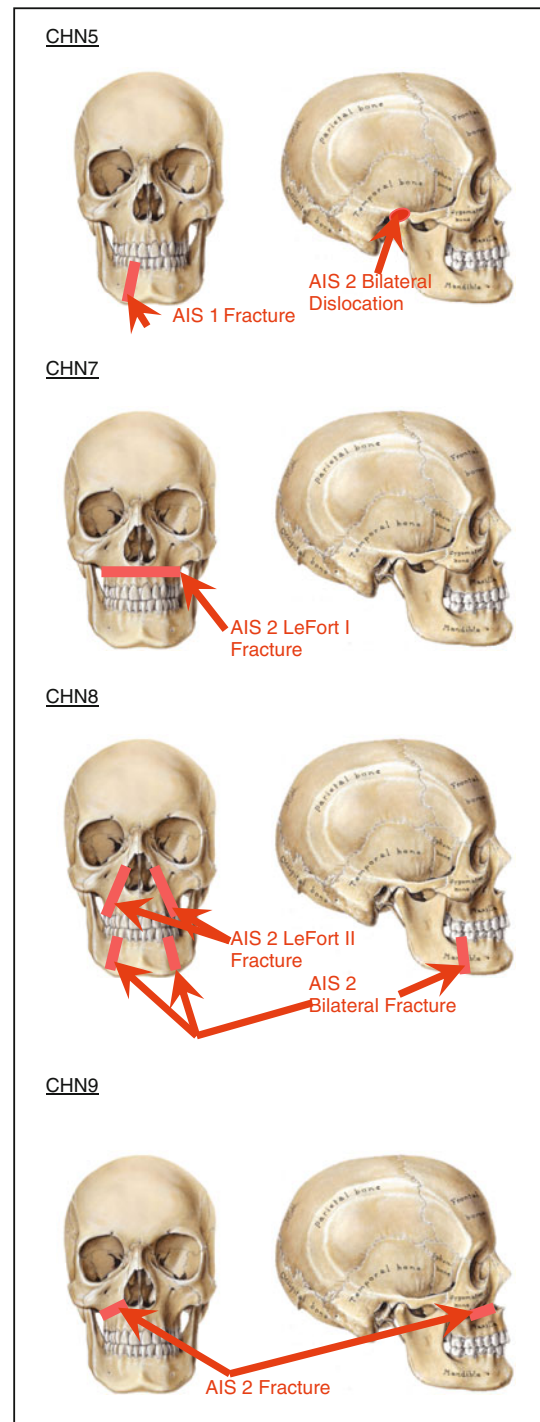
Correlation coefficients were calculated for all response, anthropometry, and age parameters. The PMHS manubrium responses were correlated more closely than chin responses to subject anthropometry. The manubrium deflection at peak force was strongly correlated to both chest breadth (0.98) and chest circumference (0.87). The manubrium peak force (0.87)

TABLE 5. Maximum forces associated with fracture/injury in PMHS chin impacts.

Subject	Test velocity (m/s)	Peak force (N)	Peak force (scaled) (N)	Injury	Energy (J)
CHN5	0.8	1503	1146	0	7.7
	1.6	2727	2078	0	30.7
	0.8	1810	1379	0	7.7
	2.0	3564	2716	0	48.0
	0.8	1566	1193	0	7.7
	2.4	3853	2936	0	69.1
	0.8	988	753	0	7.7
	2.9	4199	3199	1	100.9
CHN7	0.8	2317	1867	0	7.7
	1.6	3740	3015	0	30.7
	0.8	2356	1899	0	7.7
	2.0	5091	4104	0	48.0
	0.8	2537	2045	0	7.7
	2.4	5977	4817	0	69.1
	0.8	1809	1458	0	7.7
	2.9	6766	5454	1	100.9
CHN8	0.8	1767	1334	0	7.7
	1.6	3141	2371	0	30.7
	0.8	1609	1215	0	7.7
	2.0	3917	2957	0	48.0
	0.8	1200	906	0	7.7
	2.4	4603	3475	0	69.1
	0.8	1453	1097	0	7.7
	2.9	4823	3641	1	100.9
CHN9	0.8	1859	1428	0	7.7
	1.6	2910	2235	0	30.7
	0.8	1874	1439	0	7.7
	2.0	3412	2620	0	48.0
	0.8	1764	1355	0	7.7
	2.4	3694	2837	0	69.1
	0.8	1904	1463	0	7.7
	2.9	4976	3822	0	100.9
	0.8	1490	1145	0	7.7
	3.6	4724	3628	1	155.5

FIGURE 7. Injuries in chin fracture tolerance tests.

and compressive work (−0.84) were both strongly correlated with shoulder breadth for the six subjects. Manubrium compressive work (0.81) was also strongly correlated with chest breadth. For the chin, the force at peak deflection (−0.89) had a strong correlation with head breadth, but no other response parameter had a correlation coefficient above 0.7. Age was not a significant factor for any chin or manubrium response parameters.

From Table 1, the average chin impact velocity for 11 sled tests with different boosters was 4.4 ± 0.8 m/s. While this range is considerably higher than the 1.6-m/s PMHS test speed, it was felt that the impact energy and chin force impulse were the important parameters to replicate in the experimental conditions. The average impulse calculated from the eleven chin force–time histories was 30.1 ± 14 N s; the change in momentum for test 315-2 was 36.8 N s (24 kg × 1.54 m/s), which was between the mean and +1 standard deviation.

The kinetic energy applied (30.7 J) in the experiment was within the range of sled tests (37.7 ± 15 J) calculated from the physical head mass and chin contact velocity. In addition, the larger flexible spine noted for PMHS in other studies would result in a chin impact velocity significantly lower for PMHS than an ATD, as more energy would be absorbed by the spine before

head contact with the chest. Therefore, a lower input velocity than the HYGE sled chin velocity of the ATD is likely a better representation of what a PMHS or occupant would experience in a frontal crash.

Hopper *et al.*[5] found that an impact force of 5270 N was required for mandible fracture. The PMHS peak forces in the portion of the current study designed to derive chin stiffness ranged from 2720 to 3730

N. Craig *et al.*[2] found a mean fracture force of 1640 N for female specimens (82.5 ± 4.1 years of age) and 3830 N for male specimens (48.3 ± 19.8 years of age) when the specimen chins were loaded via drop tests aligned through the occipital condyle. All four
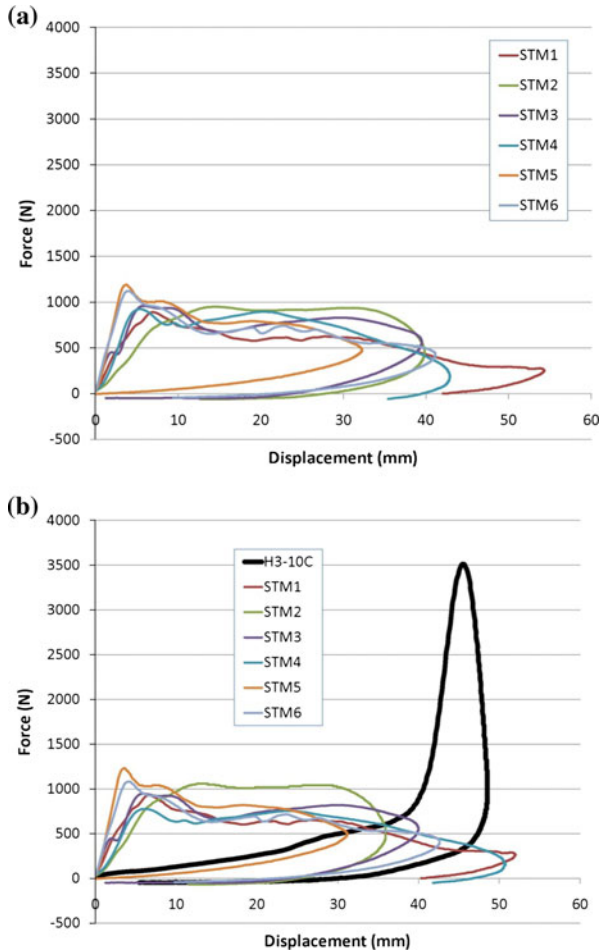

FIGURE 9. PMHS chin response corridor (red) vs. HIII-10C ATD responses.

FIGURE 8. (a) Un-scaled PMHS vs. HIII-10C manubrium impact response. (b) Scaled PMHS manubrium impact response.

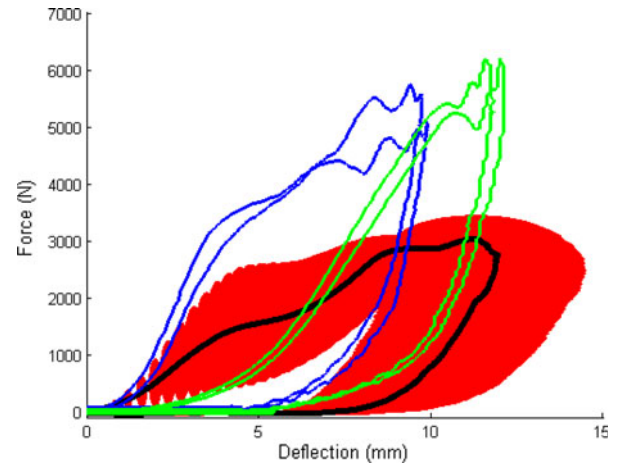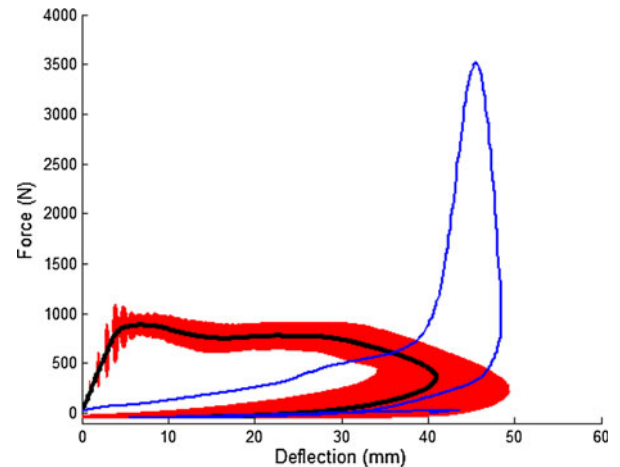FIGURE 10. Scaled PMHS manubrium corridor vs. mean HIII-10C ATD response.

TABLE 6. Manubrium test result summary (PMHS data scaled to 10YO size).

Subject	Peak force (N)	Deflection at peak force (mm)	Peak deflection (mm)	Force at peak deflection (N)	Compressive work (N m)	Hysteresis (%)	Stiffness (kN/m)
STM1	930	6.90	52.0	266	32.2	96.6	23.8
STM2	1060	13.8	35.9	578	31.3	97.6	48.6
STM3	947	5.85	40.0	573	29.5	93.5	36.9
STM4	777	5.28	50.8	173	29.4	99.8	22.8
STM5	1230	3.63	31.2	506	25.3	83.9	52.0
STM6	1080	3.83	42.6	431	28.2	92.5	31.0
PMHS Avg.	1004	6.5	42.1	421.2	29.3	94.0	35.9
PMHS Std. Dev.	155.1	3.8	8.2	167.7	2.4	5.6	12.4
HIII-10C	3510	45.5	48.5	1200	28.8	91.0	27.4
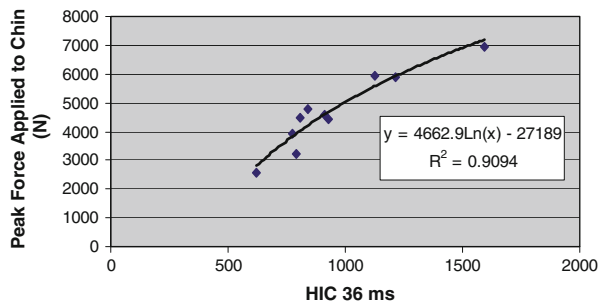
FIGURE 11. Applied chin force correlates strongly to the HIC outcome in sled testing (data from Stammen and Sullivan[16]).

specimens tested to injury in the current study were male (Table 2), indicating that the force to fracture was likely closer to 3830 N noted for male specimens in Craig *et al.* While the impact orientation in those two studies differed from the current study, the absence of fracture at the forces in the non-injurious tests is reasonable when compared to Hopper and Craig.

There was a strong relationship between the chin impact forces sustained in sled testing and the $HIC_{36\ ms}$ outcome (Fig. 11). As shown earlier, the chin impact force is calculated as the difference between the head mass times measured head acceleration and the upper neck force. Test 327-2 was removed from the dataset for this portion of the analysis because the peak acceleration experienced by the head before contact was greater than the peak head acceleration due to contact.

In the Hopper and Craig studies, energies of 11.4 and 25.5 J, respectively, were sufficient to cause multiple mandible fractures in drop tests through the head's center of gravity or occipital condyle. In the current study using fixed-head linear impacts through the anatomical *z*-axis of the chin, an input energy of 30.7 J was found to be sub-injurious and was therefore applied to develop response corridors. The mean peak force required for injury (4897 N) is within the range of Hopper (5270 N) and Craig (3830 N), but the input energy to cause injury is not consistent with those studies. This could indicate that peak force is a better correlate for mandible fracture than input energy. However, the different boundary conditions between those two studies and the current study are likely to be larger contributors to the difference. It is expected that the injury modes would be different depending on direction of impact because the structures involved in resisting the impact are different.

Using the regression equation in Fig. 11, the mean adult PMHS injury-causing impact force of 4897 N (Table 5) would be estimated to produce a $HIC_{36\ ms}$ outcome of 974 in a Hybrid III 10YO ATD in a FMVSS No. 213 booster test. A $HIC_{36\ ms}$ outcome of this magnitude is not uncommon in tests with this

ATD when the chin contacts the chest. This indicates that if the HIII-10C's spine kinematics were typical of a human child, chin/jaw/facial injuries due to this contact would be relatively common in accident data, assuming that both (a) the relative injury thresholds of 10YO children and adults are not substantially different; and (b) HIC is a viable predictor of chin/jaw/facial fracture. NASS data indicate that injuries of this type do not commonly occur to restrained older children in frontal crashes. This inconsistency indicates that chin contact (1) does not commonly occur in real crashes, (2) occurs at a different facial location in older children because of greater flexibility in the human thoracic spine than in the ATD spine, or (3) does occur but the injury risk is minimal because the older child chin and upper chest are softer than the HIII-10C's chin and upper chest. This study addresses the latter possibility that the human chin routinely contacts its own chest in some way in frontal crashes.

Several studies have demonstrated that spinal flexibility is different in Hybrid III child ATDs and humans, leading to differences of head interaction with the chest. However, some type of head–chest contact was observed to occur at higher speeds nonetheless. Lopez-Valdes *et al.*[7] showed differences in head kinematics for the Hybrid III 6YO ATD and a small adult PMHS. It was found that the PMHS chin impacted lower than the manubrium on the chest, and the PMHS head rotated more following the contact. These differences were attributed to a lack of spinal flexibility in the ATD. Sherwood *et al.*[15] used modeling to compare the kinematics of a 12YO PMHS with the Hybrid III 6YO child ATD. It was shown that spinal motion is quite different in ATD and PMHS, and increasing thoracic spine flexibility generally improves biofidelity. Ash *et al.*[1] showed similar spine motion discrepancies between a 13YO PMHS and both the Hybrid III 10YO and 5th Female ATDs. However, in this comparison, it was also observed that head kinematics and belt forces were similar between PMHS and ATD. Seacrist *et al.*[12] also showed a similar trend in ATD vs. human volunteer head and spine kinematics at low speeds. While there is some inconsistency in the chin–chest impact velocity/ orientation/location between ATD and human and it is recognized that the input conditions for the chin and manubrium impact tests are based on ATD and not on PMHS response in sled testing, the impact response of both the ATD chin and manubrium should still designed to be as biofidelic as possible.

It is expected that some reduction in HIC would result for a given booster sled test with changes to the chin, manubrium, or both. However, large variation in that HIC decrease is expected given that booster seat design can affect contact velocity of the chin, as shown by the large variation in chin contact velocities in

Table 1. It appears that both the dummy posture and booster seat design can alter the chin contact velocity/force significantly. As reported in Stammen and Sullivan[16] and NHTSA,[11] these variations can lead to large differences in HIC. It would be beneficial to investigate the relative effects of chin/manubrium stiffness, posture, and booster seat design on head acceleration.

A limitation of this study is that adult PMHS-derived forces were scaled to a HIII-10C sized person with chin forces found in sled testing with the HIII-10C dummy. Therefore, it is possible that the corridors for both the chin and manubrium in this study are skewed more toward adults than toward children if a significant difference in stiffness exists between a 10YO human and adult human. It is also possible, given the small amount of displacement in the chin test fixture, that the measured force and compression applied to the PMHS chin is slightly inaccurate. However, in PMHS testing, the amount of fixture motion is far smaller than the chin displacement, and PMHS responses in cases with near zero vs. 2.5 mm of fixture displacement were not substantially different.

This study presents data that could be used to improve ATD design. The paucity of jaw/face/chin fractures due to same occupant contact in real crash data involving older children emphasizes the need for attention toward chin-to-chest biofidelity in anthropomorphic test devices that simulate this age group.

CONCLUSIONS

- The HIII-10C dummy chin is stiffer than the scaled PMHS chin. A combination of lower durometer and increased skin thickness are recommended to improve biofidelity. The FTSS headskin appears to be closer to the scaled PMHS in both potential energy-based stiffness and peak displacement, but the peak forces are considerably higher than in the scaled PMHS.
- The HIII-10C dummy's manubrium was softer than the scaled PMHS manubrium up until around 40 mm of displacement, followed by an abrupt increase in force due to contact with the rigid ATD understructure. The HIII-10C peak force (3510 N) was over three times that of the PMHS average (1004 ± 155 N). This bimodal behavior indicates that the penetration resistance offered by the bib design is not sufficient to prevent contact with rigid ATD chest components.
- The average peak chin impact force resulting in mandible, maxillae, facial fractures, and/or TMJ dislocation was 4897 ± 1258 N ($n = 4$).

- Using the relationship between $HIC_{36\ ms}$ and peak chin impact force from the eleven sled tests along with the peak impact forces from PMHS chin testing, it was determined that $HIC_{36\ ms}$ values indicative of PMHS injury are commonly observed in HIII-10C sled testing. NASS data indicates that injuries of this type do not commonly occur to restrained older children in frontal crashes. This inconsistency indicates that chin contact (1) does not commonly occur in real crashes, (2) occurs at a different location in humans because of greater flexibility in the human thoracic spine than in the ATD spine, or (3) does occur but the injury risk is minimal because the human chin and upper chest are softer than the HIII-10C's chin and upper chest.

REFERENCES

[1]Ash, J., *et al.* Comparison of anthropomorphic test dummies with a pediatric cadaver restrained by a three-point belt in frontal sled tests. In: Enhanced Safety of Vehicles. Paper No. 09-0362, 2009.

[2]Craig, M., C. Bir, D. Viano, and S. Tashman. Biomechanical response of the human mandible to impacts of the chin. *J. Biomech.* 41:2972–2980, 2008.

[3]Craig, M., D. Viano, and C. Bir. Jaw Loading Response of Current ATDs. SAE 2009-01-0388, pp. 587–599, 2009.

[4]HIII-10C Drawing Package. http://www.regulations.gov/#!documentDetail;D=NHTSA-2005-21247-0004.

[5]Hopper, R. H., J. H. McElhaney, and B. S. Myers. Mandibular and basilar skull fracture tolerance. In: Proc. 38th Stapp Car Crash Conference. Warrendale, PA: Society of Automotive Engineers, 1994.

[6]Kallieris, D., *et al.* Comparison between child cadavers and child dummy using child restraint systems in simulated collisions. In: Presented at the 20th Stapp Car Crash Conference. SAE International, Paper No. 760815, 1976.

[7]Lopez-Valdes, F. J., *et al.* A comparison between a child-size PMHS and the Hybrid III 6 YO in a sled frontal impact. In: 53rd Annual Conference. Association for the Advancement of Automotive Medicine, pp. 237–246, 2009.

[8]Mertz, H. *et al.* The Hybrid III 10-year old dummy. In: 45th Stapp Car Crash Conference. Paper No. 2001-22-0014, 2001.

[9]Mertz, H., *et al.* Biomechanical and scaling bases for frontal and side impact injury assessment reference values.

In: 47th Stapp Car Crash Conference. Paper No. 2003-22-0009, 2003.

[10]Newman, J. A. Head injury criteria in automotive crash testing. In: Presented at 24th Stapp Car Crash Conference. SAE International, Paper No. 801317, 1980.

[11]NHTSA. Federal motor vehicle safety standards, child restraint systems; Hybrid III 10-year old child test dummy. In: Supplemental Notice of Proposed Rulemaking (NHTSA-2010-0158-0001), 2010.

[12]Seacrist, T., et al. Kinematic comparison of pediatric human volunteers and the Hybrid III 6-year-old anthropomorphic test device. In: 54th Annual Conference. Association for the Advancement of Automotive Medicine, 2010.

[13]Shaw, G., et al. Impact response of restrained PMHS in frontal sled tests: skeletal deformation patterns under seat belt loading. Stapp Car Crash J. 53:1–48, 2009.

[14]Shaw, J. M., et al. Oblique and lateral impact response of the PMHS thorax. Stapp Car Crash J. 50:147–167, 2006.

[15]Sherwood, C. P. et al. Prediction of cervical spine injury risk for the 6-year-old child in frontal crashes. In: 46th Annual Conference. Association for the Advancement of Automotive Medicine, pp. 231–247, 2002.

[16]Stammen, J., and L. Sullivan. Development of Hybrid III 6 Yr Old and 10 Yr Old Dummy Seating Procedure for Booster Seat Testing. NHTSA Docket 2007-0048-0002, 2008.